Journal of Hydroscience and Hydraulic Engineering
Vol. 27, No.1 May, 2009, 61-69



# INVERSE ANALYSIS OF ESTIMATING DISTRIBUTION OF HYDRAULIC CONDUCTIVITY AND RADIUS OF INFLUENCE USING FFT AND MULTI-WELL PUMPING TEST

By

Masahiko Saito

Research Center for Urban Safety and Security, Kobe University, Rokkodai-cho Nada, Kobe, Japan

## SYNOPSIS

The aim of this study is to determine the distribution of hydraulic conductivity and radius of influence from the results of multi-well pumping tests and the natural distribution of the piezometric head in a non-uniform confined aquifer. The inverse analysis was performed by using the Fast Fourier Transform(FFT) and the constrained simplex method. These findings showed that the method presented here can estimate the mean value of hydraulic conductivity and the radius of influence more accurately than the conventional method by using an analytical model of aquifer flow. The distributions of hydraulic conductivity were well reproduced except for the case where the heterogeneity of hydraulic conductivity was not reflected in the distribution of drawdown and piezopmetric head.

## INTRODUCTION

Knowledge of local hydraulic conductivity is essential when considering any problem concerned with groundwater or seepage flow. Hydraulic conductivity is most commonly determined through laboratory measurements of samples and in-situ pumping tests. Laboratory tests involve taking samplings from the observation points and are thus exclusively a local measurement method, whereas in-situ pumping tests provide an average value of hydraulic conductivity in the vicinity of the pumping well. As soil is heterogeneous, the hydraulic conductivity is most likely to exhibit substantial spatial variation. To construct an accurate model of groundwater and permeability, it is therefore necessary to develop a model that incorporates the spatial variability of such parameters.

Researchers have tried to develop methods for estimating the spatial distribution of hydraulic conductivity by inverse analysis of observed groundwater levels or piezometric heads in locations where observations are convenient. This approach is useful for estimating the spatial distribution in hydraulic conductivity (Carrera and Neuman (1), Okuno and Suzuki (2), Honjo et al.(3), Takeshita et al.(4)). Conventional procedures usually divide the region of interest into smaller sub-domains and determine the representative hydraulic conductivity for each sub-domain. It is inevitable that the estimated hydraulic conductivity distributions are somewhat dependent on the number of sub-domains taken and the pattern of domain division.

An alternative spatial distribution model based on a stochastic fractal model involving a density function of the form $f^{-\zeta}$ was recently proposed (Saito and Kawatani (5),(6),(7)), and such an approach has been shown to allow easy modeling of the characteristics of the spatial distribution of hydraulic conductivity in the field. Furthermore, this method allows the spatial distribution of hydraulic conductivity to be expressed as the superposition of waveforms.

In the present research, the $f^{\zeta}$ model is applied to the analysis of a planar two-dimensional (2D) confined aquifer. The distributions of drawdown from the aquifer obtained by means of a multi-well pumping test and of piezometric head under natural conditions are treated simultaneously in an attempt to develop a method for estimating the spatial distribution and radius of influence in the form of a continuity by superimposing 2D periodic functions on the Fast Fourier Transform (FFT). The practical applicability of this approach is will be discussed in the next section.

## GOVERNING EQUATION

The governing equation for steady-state seepage flow across a planar 2D confined aquifer due to the withdrawal of water from a well is given according to the continuity equation and Darcy's Law as follows :

$$\frac{\partial}{\partial x}\left(kB\frac{\partial h}{\partial x}\right)+\frac{\partial}{\partial y}\left(kB\frac{\partial h}{\partial y}\right)=Q_w\delta(x-x_w,y-y_w) \tag{1}$$

where, $x$ and $y$ are spatial coordinates, $h$ is the piezometric head, $k$ is the hydraulic conductivity, $B$ is the thickness of the aquifer, $Q_w$ is the pumping rate, $(x_w, y_w)$ are the pump coordinates, and $\delta$ is the delta function.

The boundary condition for pressure is defined by

$$h=h_b \tag{2}$$

the boundary condition of prescribed flux is given by

$$-\left(kB\frac{\partial h}{\partial x}n_x+kB\frac{\partial h}{\partial y}n_y\right)=q_b \tag{3}$$

where $q_b$ is the flow rate per unit length of external boundary, and $n_x$ and $n_y$ are the components of the unit vector normal to the boundary.

## FFT-BASED INVERSE ANALYSIS

The observed values of drawdown while pumping at the $m$ observation points and the distribution of piezometric heads under natural conditions in the same locations were employed in the inverse analysis, constituting a total of $2m$ observed values. It is assumed that the hydraulic conductivity distribution in a heterogeneous field is characterized by the following spectral density function (Saito and Kawatani (5),(6),(7)):

$$S(|\boldsymbol{f}|) \propto |\boldsymbol{f}|^{-\zeta} \tag{4}$$

where $\boldsymbol{f}$ denotes a wave number vector, $S(|\boldsymbol{f}|)$ is a spectral density function, and $\zeta$ is a parameter expressing the spatial correlation. In a 2D model, $\zeta \approx 2.0$.

In the inverse analysis, the hydraulic conductivity distribution is expressed by the sum of $n$ waves. The spatial distribution of log $k$ is expressed by using the wavenumber vector $(\boldsymbol{f}^{(i)}=(f^{(i)}_x, f^{(i)}_y))$ as follows.

$$\log k(x,y) = \sum_{i=1}^{n} W^{(i)}(x,y) \tag{5}$$

$$W^{(i)}(x,y) = a^{(i)} \sin\left\{\frac{2\pi}{L}\left(f^{(i)}{}_x x + f^{(i)}{}_y y\right) + \varphi^{(i)}\right\} \tag{6}$$

where, $a^{(i)}$ is the amplitude of $\boldsymbol{f}^{(i)}$ and is determined by Eq. (4), $L$ is a representative value of the size of the domain, and $\varphi^{(i)}$ is the phase of $\boldsymbol{f}^{(i)}$. The inverse transformation of the FFT is employed to perform these calculations.

A total of $n$ $\varphi^{(i)}$ functions, the mean of log $k$ ($=\mu_k$), and the standard deviation of log $k$ ($=\sigma_k$) are estimated from the inverse analysis. In addition, the radius of influence $R$ is usually unknown and must be estimated. Therefore, the constraint of $m$ is given by $2m > n + 3$.

The constrained simplex method is employed to search for parameter values by using the following minimizing objective function:

$$g(\varphi_1, \varphi_2, \cdots, \varphi_n, \mu_k, \sigma_k, R) = \sum_{j=1}^{2m} \frac{\left\{h_c^{(j)} - h_o^{(j)}\right\}^2}{\left|h_o^{(j)}\right|} \tag{7}$$

where, $h_c^{(j)}$ and $h_o^{(j)}$ are the calculated and observed values of the $j$th piezometric head value, respectively.

## ANALYTICAL CONDITIONS

*Observed values (Forward analysis)*

The observed values were processed by the finite element method (FEM) forward analysis. Figures 1 and 2 show the analytical conditions and observation points at which the piezometric head was obtained under natural conditions and during the pumping test. The analytical region was 500 m × 500 m in size (i.e., $L$ = 500 m), and the heads at the upstream and downstream ends were approximated at 5 m and 0 m. The array of elements was 256×256 in size, and the thickness $B$ of the aquifer was assumed to be uniformly 1 m. The pumping well was located at $x$ = 250 m, $y$ = 250 m, and the drawdown was set to 10 m. The radius of influence $R$ was assumed to be 220 m based on the maximum distance at which distinguishable head loss was observed. The drawdown was assumed here to be 0 m. The pumping rate $Q_w$ was used as an input condition in the inverse analysis. Observations were taken at 16 different points, surrounding the pumping well ($m$ = 16).

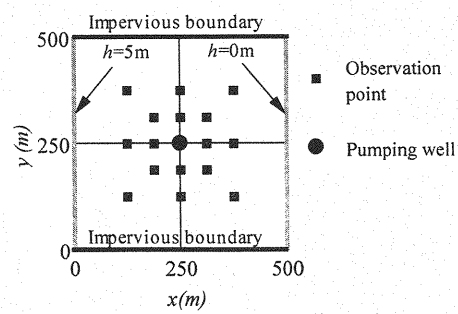


Figure 1: Analytical conditions and observation points under natural conditions

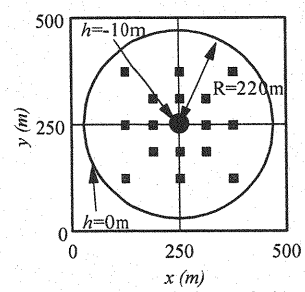


Figure 2: Analytical conditions and observation points during pumping

Figure 3 shows an example of the hydraulic conductivity distribution (random number sequence A) produced by using Eq. (4). This distribution was created with a resolution of 512×512 (i.e., on a 1000 m × 1000 m region). A 256×256 point array was then removed from this for the subsequent analysis. A distribution including a half-frequency component was then created. Values of $\mu_k = -3.0$ (mean of $\log_{10}k$, units of $k$ are cm/s) and $\sigma_k = 0.4$ were adopted. Figure 4 shows the hydraulic conductivity distribution of the portion of the area shown in Fig. 3 within the radius $R$ of the well.

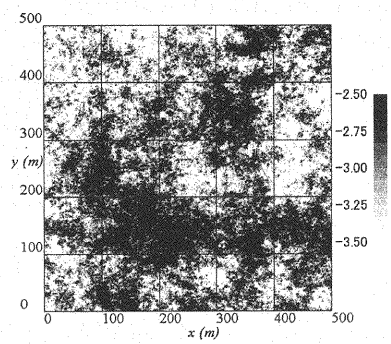


Figure 3: Example of generated hydraulic conductivity distribution ($\log_{10} k$, where $k$ is in cm/s) under natural conditions (Random Seq A)

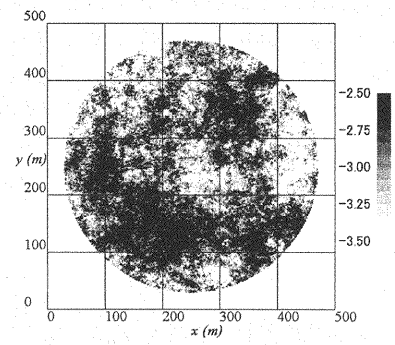


Figure 4: Example of generated hydraulic conductivity distribution ($\log_{10} k$, where $k$ is in cm/s) during pumping(Random Seq A)

*Inverse analysis*

Ten estimates of the hydraulic conductivity distribution were produced by inverse analysis using different random number series. The overall trend in the hydraulic conductivity distribution displayed mainly low-frequency components, but also some low-amplitude high-frequency components. The dense arrangement of the observation points made it possible to reproduce the finer fluctuations. However, this was not very practical, and also requires the use of higher frequencies: for $N$ frequency components, the required number of estimation parameters grows according to $n = 2N(N+1)$. Here, only the low-frequency ($N = 2$) portions are used, with the objective to reproduce the tendencies of the overall distribution. A total of six wavenumber vectors were used in the inverse analysis: $\boldsymbol{f}^{(1)} = (0,1)$, $\boldsymbol{f}^{(2)} = (0,2)$, $\boldsymbol{f}^{(3)} = (1,1)$, $\boldsymbol{f}^{(4)} = (1, 2)$, $\boldsymbol{f}^{(5)} = (2,1)$, and $\boldsymbol{f}^{(6)} = (2,2)$. The following 6 orthogonal waveforms with the same corresponding magnitude $|\boldsymbol{f}^{(i)}|$ were also used, for a total of 12: $\boldsymbol{f}^{(7)} = (1,0)$, $\boldsymbol{f}^{(8)} = (2,0)$, $\boldsymbol{f}^{(9)} = (1,-1)$, $\boldsymbol{f}^{(10)} = (2,-1)$, $\boldsymbol{f}^{(11)} = (1,-2)$, and $\boldsymbol{f}^{(12)} = (2,-2)$. The parameters to be estimated are the phases $\varphi^{(i)}$ of the 12 waves, $\mu_k$, $\sigma_k$, and the radius of influence $R$ (a total of 15 quantities).

No high-frequency fluctuations were apparent, since low frequencies were used for the inverse analysis. The mesh size shown in Fig. 1 was used in a 32×32 element array.

## RESULTS AND DISCUSSION

*Comparison of the Thiem's equation with inverse analysis*

The hydraulic conductivity and radius of influence were estimated from the Thiem's equation (Eq. (8)) using the drawdown from two locations at different distances from the pumping well.

$$T = kB = \frac{Q_w}{2\pi(s_1 - s_2)} \log_e \left( \frac{r_2}{r_1} \right) \tag{8}$$

where $T$ is the transmissivity, $r_1$ and $r_2$ are the respective distances of the observation well from the pumping well, and $s_1$ and $s_2$ are the respective drawdown in the observation well. These parameters were estimated by using the data at two points each in 8 radial directions from the pumping well. The hydraulic conductivity was defined as the geometric mean of the 8 estimated values, and the radius of influence was defined as the arithmetic mean. The obtained values of the hydraulic conductivity and the radius of influence were then compared with the mean hydraulic conductivity $\mu_k$ and $R$ determined by the inverse analysis. Table 1 compares the hydraulic conductivity distributions predicted by the Thiem's equation and the inverse analysis for the 10 distributions, with input values of $\mu_k$ = -3.0 ($k_m$=1.0 × $10^{-3}$cm/s) and $R$ = 220 m. Although some values estimated from the Thiem's equation are quite close to the actual values, on the whole, the predictions by the inverse analysis are closer to the input values.

Table 1: Comparison of the Thiem equation and inverse analysis

| | Mean value of hydraulic conductivity (×$10^{-3}$ cm/s) | | | Radius of Influence (m) | | |
|---|---|---|---|---|---|---|
| Random Seq. | Thiem's Equation | (max, min) | Inverse Analysis | Thiem's Equation | (max, min) | Inverse Analysis |
| A | 1.58 | (1.04, 2.43) | 1.14 | 259 | (187, 305) | 236 |
| B | 0.86 | (0.60, 1.45) | 1.01 | 223 | (194, 325) | 228 |
| C | 1.03 | (0.84, 1.46) | 1.04 | 218 | (185, 248) | 231 |
| D | 0.99 | (0.58, 1.35) | 0.89 | 205 | (166, 247) | 221 |
| E | 0.83 | (0.62, 1.10) | 1.00 | 212 | (182, 246) | 236 |
| F | 1.06 | (0.85, 1.48) | 1.06 | 209 | (183, 253) | 217 |
| G | 1.20 | (0.93, 1.71) | 1.26 | 228 | (172, 297) | 230 |
| H | 1.45 | (0.99, 1.87) | 1.09 | 258 | (218, 304) | 228 |
| I | 1.28 | (1.07, 1.52) | 1.04 | 242 | (199, 283) | 237 |
| J | 1.62 | (1.28, 2.50) | 0.95 | 299 | (239, 481) | 233 |
| Mean | 1.16 | | 1.04 | 235 | | 230 |

*Estimates of hydraulic conductivity distribution (Part 1; successful attempts)*

Figure 5 shows the hydraulic conductivity distribution estimated Fig.4 by the inverse analysis. The observations are not reproduced very well in the vicinity of the pumping well, however, the locations with the highest hydraulic conductivity are resolved. Figure 6 compares the observed and predicted piezometric heads. The results fall consistently on a 1:1 line, indicating an excellent reproduction of that parameter.

Figures 7 – 10 compare the magnitudes of the velocity vectors (= $|V| = \sqrt{v_x^2 + v_y^2}$ ) under natural conditions and during pumping. Although the water paths are not very accurate, it appears that from these results that the general characteristics of the flow velocity distribution are reproduced well, providing sufficient information to help researchers understand the phenomenon of groundwater flow.

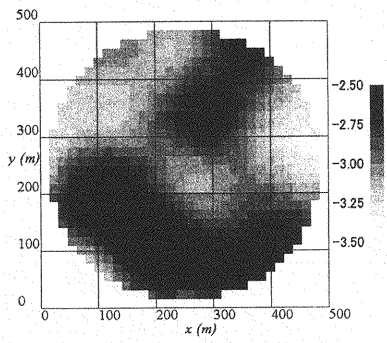


Figure 5: Estimated hydraulic conductivity distribution ($\log_{10}k$, where $k$ is in cm/s; random seq. A)

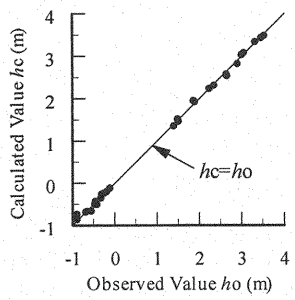


Figure 6: Reproduction of piezometric head

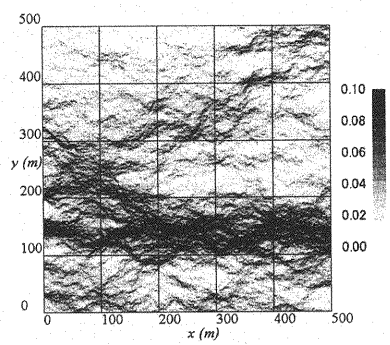


Figure 7: $|V|$ distribution (cm/h) under natural conditions (forward analysis)

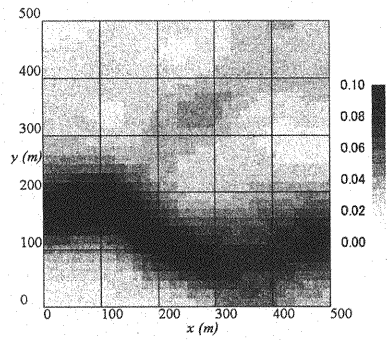


Figure 8: $|V|$ distribution (cm/h) under natural conditions (inverse analysis)

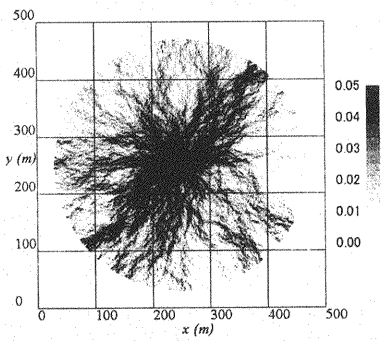


Figure 9: $|V|$ distribution (cm/h) during pumping (forward analysis)

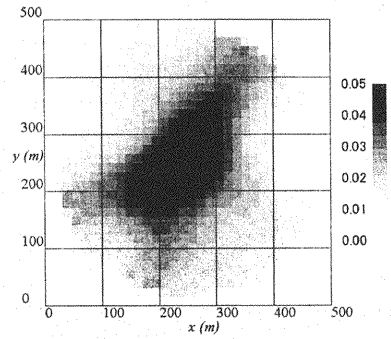


Figure 10: $|V|$ distribution (cm/h) during pumping (inverse analysis)

Figures 11 and 12 show the hydraulic conductivity distributions for the forward analysis and estimated hydraulic conductivity distribution developed from another random number sequence (sequence D). These cases also generally reproduce the characteristics of the original distributions, providing evidence of the effectiveness of the inverse analysis, and are presented here as instances of the success of this method.

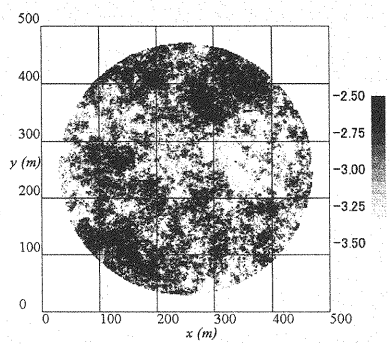


Figure 11: Hydraulic conductivity distribution ($\log_{10}$, where $k$ is in cm/s $k$; random seq. D)

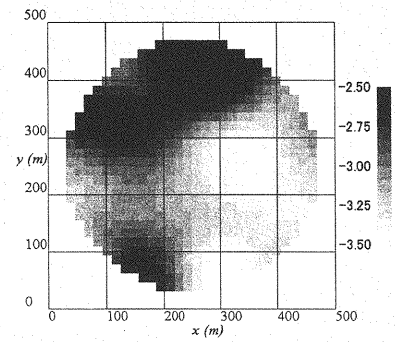


Figure 12: Estimated hydraulic conductivity distribution ($\log_{10}k$, where $k$ is in cm/s; random seq. D)

*Estimates of hydraulic conductivity distribution (Part 2; unsuccessful attempts)*

Figures 13 and 14 show the hydraulic conductivity distribution created from another random number sequence (sequence F) and the estimated distribution respectively. As is clearly seen from Fig. 14, the model produced relatively uniform values and failed to reproduce the real situation well. Figure 15 shows a good reproduction of the piezometric head distribution, where the estimated values corresponded closely to the measured values, tracing a nearly straight line on the coordinate plane, as seen above in Fig. 6.

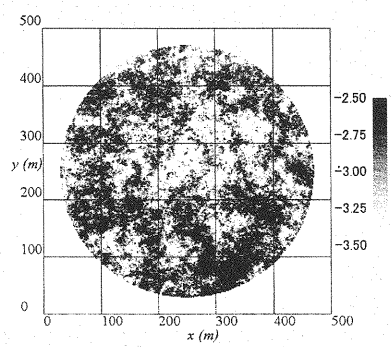


Figure 13: Hydraulic conductivity distribution ($\log_{10}k$, where $k$ is in cm/s; random seq. F)

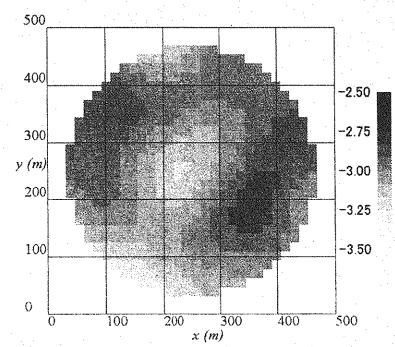


Figure 14: Estimated hydraulic conductivity distribution ($\log_{10}k$, where $k$ is in cm/s; random seq. D)

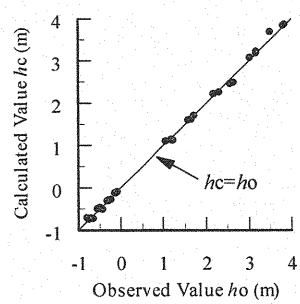


Figure 15: Reproduction of observed piezometric head

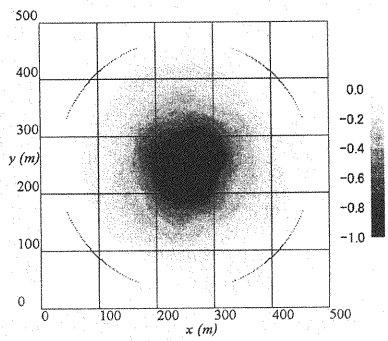


Figure 16: Distribution of piezometric head (m) (forward analysis; random seq. F)

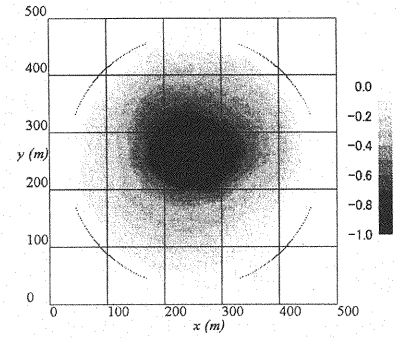


Figure 17: Distribution of piezometric head(m) (forward analysis; random seq. A)

Figure 16 illustrates the head distribution during pumping, having basically a concentric circular pattern. The heterogeneity of the hydraulic conductivity distribution was almost nowhere reflected in the head distribution. In contrast, Fig. 17 shows a successful example (random number sequence A) of modeling the piezometric head distribution during pumping. The obvious influence of heterogeneity on the distribution can be seen in the form of distorted isobars. Accordingly, even though the field is heterogeneous, when the head distribution is close to homogeneous, as observed in random number sequence F, it is impossible to reproduce the hydraulic conductivity distribution using reproductions of observed piezometric head levels by inverse analysis.

## CONCLUSIONS

This study used a $f^{\zeta}$ model for the spectral density function of the spatial hydraulic conductivity distribution to estimate the spatial hydraulic conductivity distribution continually from the piezometric head data which was obtained both in a natural condition and a multi-well pumping test.

Findings of this study can be summarized as follows:

1. A comparison of the Thiem equation with estimates by the inverse analysis revealed that inverse analysis provides more accurate estimates of the mean of the hydraulic conductivity and radius of influence than the Thiem equation.

2. The present method cannot provide continuous reproduction of the hydraulic conductivity distribution, as long as the distribution of piezometric head displays a similar level of heterogeneity to that of the hydraulic conductivity.

3. When the heterogeneity of the permeability is not well reflected in the distribution of piezometric head, the estimates become nearly uniform. Under such conditions, it is not possible to estimate the hydraulic conductivity distribution on the basis of observed hydraulic conductivities alone.

## REFERENCES

1. Carrera, J. and Neuman, S. P.: Estimation of aquifer parameters under transient and steady state condition,
1: Maximum likelihood method incorporating prior information, Water Resources Research, Vol.22, No.2, pp.199-210, 1986.
2: Uniqueness, stability, and solution algorithms, Water Resources Research, Vol.22, No.2, pp.211-227, 1986.
3: Application to synthetic and field data, Water Resources Research, Vol.22, No.2, pp.228-242, 1986.

2. Okuno, T. and Suzuki, M.: Parameter identification in unconfined aquifer using extended Kalman filter algorithm, Journal of Geotechnical Engineering, No.469/III-23, pp.93-102, 1993. (in Japanese)
3. Honjo, Y., Fukui, H. and Ogawa, S.: Inverse analysis of a regional groundwater flow model by extended bayesian method: In case of steady flow data, Journal of Geotechnical Engineering, No.535/III-34, pp.93-102, 1996. (in Japanese)
4. Takeshita, Y., Kohno, I. and Yasui, K.: Determination of the hydraulic properties of a multilayered aquifer from pumping test data using genetic algorithms, Proceedings of the 3rd International conference on CALIBRATION AND RELIABILITY IN GROUNDWATER MODELING, pp.229-235, 1999.
5. Saito, M. and Kawatani, T.: Theoretical Study on Spatial Distribution of Hydraulic Conductivity, Journal of Geotechnical Engineering, No.645/III-50, pp.103-114, 2000. (in Japanese)
6. Saito, M. and Kawatani, T.: Study on Applicability of Geostatistical Models of Hydraulic Conductivity, Journal of Geotechnical Engineering, No.694/III-57, pp.245-258, 2001. (in Japanese)
7. Saito, M. and Kawatani, T.: Simple method for generation of 1-D and 2-D random permeability field by using stochastic fractal model, Proceedings of the 4th International conference on CALIBRATION AND RELIABILITY IN GROUNDWATER MODELING, Vol.1, pp.176-179, 2002.

## APPENDIX – NOTATION

The following symbols are used in this paper:

$a$ = amplitude of $\boldsymbol{f}$;
$B$ = thickness of aquifer;
$\boldsymbol{f}$ = wave number vector;
$h$ = piezometric head;
$h_c$, $h_o$ = calculated and observed value of piezometric head;
$k$ = hydraulic conductivity;
$k_m$ = geometric mean of $k$;
$L$ = representative value of the size of the domain;
$m$ = number of observation points;
$n$ = number of waves;
$n_x$, $n_y$ = components of the unit vector normal to the boundary;
$N$ = number of frequency components;
$q_b$ = flow rate per unit length of external boundary;
$Q_w$ = pumping rate;
$r_1$ , $r_2$ = distances of the observation well from the pumping well;
$R$ = radius of influence;
$s_1$ , $s_2$ = drawdown in the observation well;
$T$ = transmissivity;
$v_x$, $v_y$ = components of the velocity vector;
$\boldsymbol{V}$ = velocity vector;
$x$, $y$ = spatial coordinates;
$\varphi$ = phase of $\boldsymbol{f}$;
$\mu_k$ = $\log_{10} k_m$;
$\sigma_k$ = standard deviation of log $k$;
$\zeta$ = parameter expressing the spatial correlation;

(Received Jul 31, 2008 ; revised Dec 05, 2008)